ORIGINAL RESEARCH

Effects of Low Endothelial Shear Stress After Stent Implantation on Subsequent Neointimal Hyperplasia and Clinical Outcomes in Humans

Koki Shishido, MD; Antonios P. Antoniadis, MD, PhD; Saeko Takahashi, MD; Masaya Tsuda, MD; Shingo Mizuno, MD; Ioannis Andreou, MD, PhD; Michail I. Papafaklis, MD, PhD; Ahmet U. Coskun, PhD; Caroline O'Brien, PhD; Charles L. Feldman, ScD; Shigeru Saito, MD; Elazer R. Edelman, MD, PhD; Peter H. Stone, MD

***Background*—**In-stent hyperplasia (ISH) may develop in regions of low endothelial shear stress (ESS), but the relationship between the magnitude of low ESS, the extent of ISH, and subsequent clinical events has not been investigated.

***Methods and Results*—**We assessed the association of poststent ESS with neointimal ISH and clinical outcomes in patients treated with percutaneous coronary interventions (PCI). Three-dimensional coronary reconstruction was performed in 374 post-PCI patients at baseline and 6 to 10 months follow-up as part of the PREDICTION Study. Each vessel was divided into 1.5-mm-long segments, and we calculated the local ESS within each stented segment at baseline. At follow-up, we assessed ISH and the occurrence of a clinically indicated repeat PCI for in-stent restenosis. In 246 total stents (54 overlapping), 100 (40.7%) were bare-metal stents (BMS), 104 (42.3%) sirolimus-eluting stents, and 42 (17.1%) paclitaxel-eluting stents. In BMS, low ESS post-PCI at baseline was independently associated with ISH (β=1.47 mm^2 per 1-Pa decrease; 95% CI, 0.38–2.56; P<0.01). ISH was minimal in drug-eluting stents. During follow-up, repeat PCI in BMS was performed in 21 stents (8.5%). There was no significant association between post-PCI ESS and in-stent restenosis requiring PCI.

***Conclusions*—**Low ESS after BMS implantation is associated with subsequent ISH. ISH is strongly inhibited by drug-eluting stents. Post-PCI ESS is not associated with in-stent restenosis requiring repeat PCI. ESS is an important determinant of ISH in BMS, but ISH of large magnitude to require PCI for in-stent restenosis is likely attributed to factors other than ESS within the stent. **(*J Am Heart Assoc*. 2016;5:e002949 doi: 10.1161/JAHA.115.002949)**

Key Words: imaging • in-stent restenosis • neointimal hyperplasia • percutaneous coronary intervention • shear stress

Percutaneous coronary intervention (PCI) with stent implantation is a major therapeutic strategy in patients with clinically evident coronary artery disease. However, in-stent restenosis (ISR) is the main limitation of coronary stenting, especially for bare-metal stents (BMS). The predominant mechanism of ISR is neointimal in-stent hyperplasia (ISH),[1] resulting from proliferation and migration of vascular smooth muscle cells (VSMCs). Drug-eluting stents (DES) reduce neointimal ISH through inhibited VSMC growth and delayed re-endothelialization and healing. The different magnitude of ISH between BMS and DES has been demonstrated in large-scale studies.[2,3]

Various factors influence ISH, such as arterial injury by stent struts[4] and endothelial dysfunction.[5] In addition, local hemodynamic factors, in particular, endothelial shear stress (ESS), are important determinants of vascular biology and atherosclerosis,[6] eliciting multiple effects on endothelial cells and VSMCs.[7] Whereas early studies on the association between ESS magnitude and ISH were controversial,[8] most recent investigations demonstrated an inverse relationship between ESS and ISR after BMS implantation.[9,10] In DES, only a few similar studies were conducted, without reaching definitive conclusions.[11–13] Therefore, the effect of low ESS within the stent on subsequent clinical events in humans requires further investigation. Furthermore, stent overlap is associated with increased ISR and lumen loss regardless of stent type.[14] Flow within the stents may be affected by

From the Cardiovascular Division, Brigham and Women's Hospital, Harvard Medical School, Boston, MA (K.S., A.P.A., I.A., M.I.P., C.L.F., E.R.E., P.H.S.); Department of Cardiology, Shonan Kamakura General Hospital, Kamakura, Japan (K.S., S.T., S.M., S.S.); Hakodate Municipal Hospital, Hakodate, Japan (M.T.); Mechanical and Industrial Engineering, Northeastern University, Boston, MA (A.U.C.); Institute for Medical Engineering and Science, Massachusetts Institute of Technology, Cambridge, MA (C.O'B., E.R.E.).

Correspondence to: Peter H. Stone, MD, Cardiovascular Division, Brigham and Women's Hospital, Harvard Medical School, 75 Francis St, Boston, MA 02115. E-mail: pstone@partners.org

Received January 11, 2016; accepted July 22, 2016.

overlapping segments, and the relationship between the hemodynamics inside overlapping stents and in-stent outcomes have not been examined in clinical settings.

This study aims to assess the association of immediate post-PCI ESS with the anatomic natural history in stented regions over a 6- to 10-month period and clinical outcomes arising from ISR in a large patient cohort undergoing PCI for an acute coronary syndrome (ACS). The analysis was based on data from the Prediction of Progression of Coronary Artery Disease and Clinical outcome Using Vascular Profiling of Shear Stress and Wall Morphology (PREDICTION) Study with focus on the investigation of stent outcomes.

Methods

Study Population

The PREDICTION study is a multicenter investigation at 17 clinical sites in Japan to identify the detailed coronary hemodynamic and plaque characteristics at baseline (BL) that would predict future cardiac events in 1-year follow-up (FU). The primary PREDICTION analysis was reported previously.[15] In brief, 506 Japanese patients with ACS who underwent PCI of all culprit lesions were enrolled. Patients underwent intracoronary vascular profiling (VP) with intravascular ultrasound (IVUS) and angiography of all major coronary arteries at the time of PCI. A large subset of consecutive, unselected patients underwent routine FU VP after 6 to 10 months to assess the anatomic natural history in relation to antecedent vascular characteristics. All patients had clinical FU at 1 year. This report focuses on stent characteristics and stent outcomes.

Three-Dimensional Reconstruction of Coronary Arteries

The methods of intracoronary VP have been previously described.[16–19] In brief, IVUS and biplane coronary angiography were utilized to create an accurate three-dimensional (3D) representation of the coronary artery. IVUS was performed with automated pullback at 0.5 mm/s. The lumen and outer vessel wall were reconstructed from segmented end-diastolic IVUS frames. Coronary blood flow was calculated directly from the time required for the volume of blood contained within the portion of the artery under study to be displaced by contrast material in coronary angiography.[20] The stent was considered only as a zone along the arterial wall and not as a solid-body geometry. We did not investigate the contours or geometry of individually modeled stents. The 3D geometry of ISH was taken as the difference between the stented region and the lumen area. ESS within the stented region at the luminal surface of the artery was calculated as the product of blood viscosity (calculated from the measured hematocrit) and the gradient of blood velocity at the wall. The process of data acquisition and analysis are highly reproducible.[17] In the computational fluid dynamics (CFD) simulations, we impose measured blood flow to pass through the reconstructed geometry under nonslip condition (zero velocity) on the arterial walls. Mathematical model uses linear momentum (the Navier-Stokes) equations to find the velocity distribution at the faces of computational cells. The CFD model also has shear rates (velocity gradients) in every spatial direction to solve the governing equations. Thus, the gradient of blood velocity at the wall is determined from the shear rate at the computational cell on the wall, as published before.[17] More specifically, magnitude of the shear rate is defined based on the strain rate tensor as follows:

$$\dot{\gamma}\sqrt{\frac{1}{8}\sum_{i=1}^{3}\sum_{j=1}^{3}\left(\frac{u_j}{x_i}+\frac{u_i}{x_i}\right)^2}$$

Here, i, j=1, 2, 3 are the 3 coordinate directions, and x_i and u_i are, respectively, the dimension and velocity in the direction i. $\dot{\gamma}$ above becomes velocity gradient in the normal direction to the wall. In this study, we defined ESS as a measure of flow within the stented portion of the artery and specific stent geometries were not included into our CFD calculations.

Study Assessments

Each 3D reconstructed artery was divided into consecutive 1.5-mm segments. Whereas 3-mm segments had been used in the analysis of the PREDICTION study,[15] we selected 1.5-mm segments to investigate the stented regions because the stented segments are considerably shorter than the native coronary arteries and a finer resolution for all measurements would be required to precisely capture the local characteristics of blood flow and regional vascular anatomy within a stented region. The contours of the stented region were identified by selecting the stent struts on the IVUS image and connecting them with a straight line, which was then smoothed along the longitudinal course of the stented region. Within each 1.5-mm segment, we assessed local ESS following successful PCI at BL. The same 3D coronary artery segments were evaluated at FU 6 to 10 months later. Anatomic matching at BL and FU was accomplished by using fixed anatomic landmarks, multiple arterial branches, and stent edges as reference fiducial points.

Within each 3D 1.5-mm stent segment, we assessed local ESS and vessel/lumen characteristics. Each stented segment was characterized by local predominant ESS value (defined as the minimum averaged ESS value over 90 arcs in the arterial circumference). Vessel area, lumen area, plaque area, and ISH

area were measured for each stented segment at both BL and FU. Stented area was calculated as lumen area plus ISH area. Plaque area behind the stent was calculated as vessel area minus stent area, and the plaque burden behind the stent was calculated as the plaque area behind the stent divided by the vessel area. Percent ISH (%ISH) area at FU was calculated as (ISH area/stent area $\times 100$). Change in each parameter (delta) was calculated as the respective FU measurement

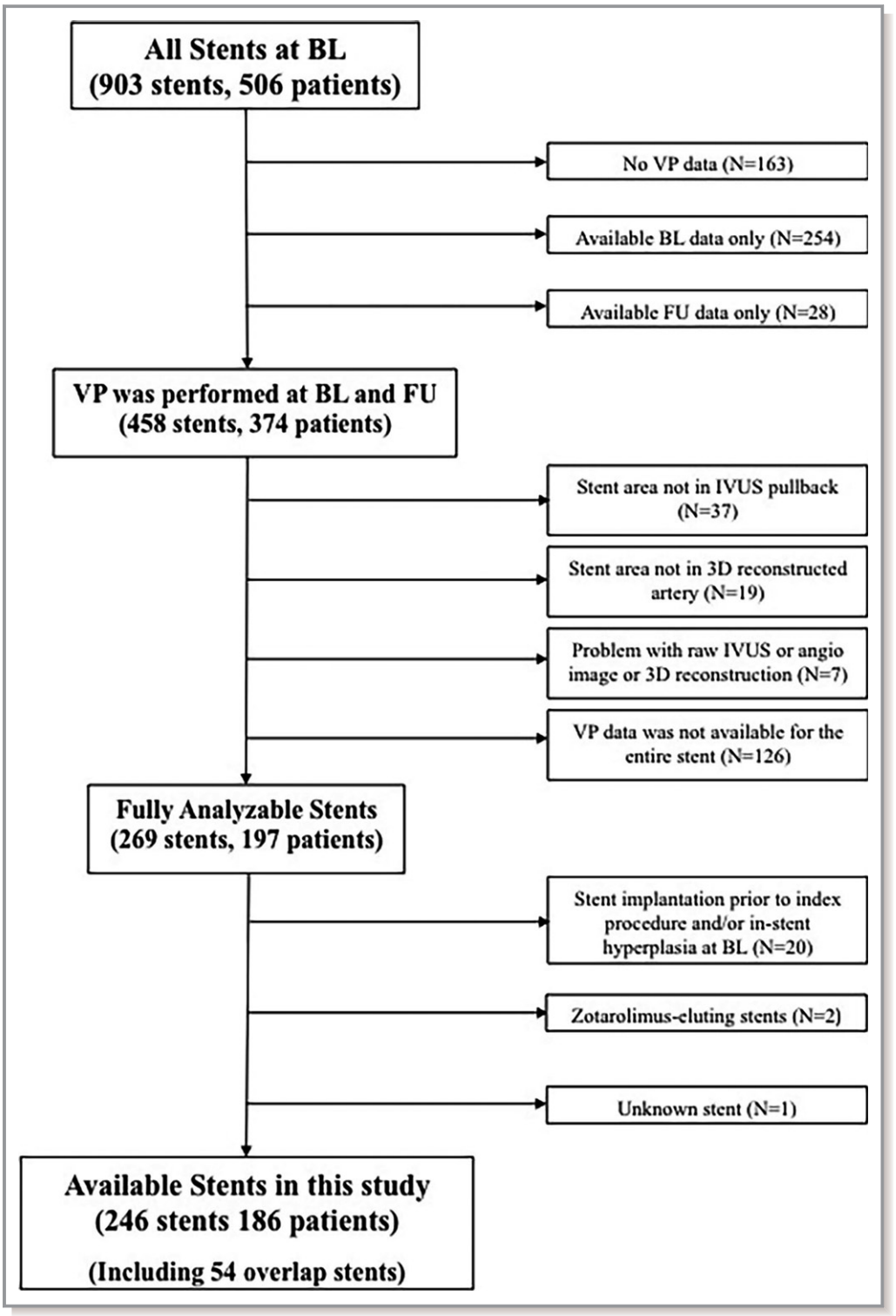

Figure 1. Study flow chart. 3D indicates three-dimensional; BL, baseline; FU, follow-up; IVUS, intravascular ultrasound; VP, vascular profiling.

Table 1. Baseline Demographics

Characteristic	Available Patients (N=186)
Female sex, n (%)	39 (21.0)
Age, y	65 (58–72)
Hypertension, n (%)	112 (60.2)
Dyslipidemia, n (%)	
LDL >100 mg/dL, n (%)	139 (74.7)
HDL <40 mg/dL, n (%)	80 (43.0)
Cigarette smoking (within last 2 years), n (%)	97 (52.2)
Diabetes mellitus, n (%)	59 (31.7)
Insulin dependent, n (%)	5 (2.7)
Family history of premature CAD, n (%)	9 (4.8)
History of myocardial infarction, n (%)	9 (4.8)
History of PCI, n (%)	13 (7.0)

Continuous variable data are presented as median (interquartile range). The definition for hypertension was blood pressure >140/90 mm Hg. CAD indicates coronary artery disease; HDL, high-density lipoprotein; LDL, low-density lipoprotein; PCI, percutaneous coronary intervention.

minus BL measurement. Percent change in each parameter (% delta) was calculated as (change in parameter/value of parameter at BL $\times$100). Overlapping stents were defined as stents featuring an overlapping stent zone of at least 1.5 mm in length.

In terms of clinical outcomes, we identified the BL stent areas that were treated by subsequent PCI for ISR at FU. We investigated the impact of BL stent characteristics on ISH and clinical outcomes in BMS. Furthermore, we similarly examined the anatomical outcomes in overlapping versus nonoverlapping stents. Cases of in-stent thrombosis were very infrequent and therefore not included in this analysis.

Statistical Analysis

Continuous variables are presented as the mean$\pm$SD or median and interquartile ranges (IQRs) as appropriate. To correct for the systematic error introduced by the clustering of stents within patients, several statistical methods were used. First, to investigate the association of continuous variables (eg, BL vessel area) with categorical variables (eg, stent type), we used mixed-effects ANOVA with the patient and stent defined as random effects. Probability values were adjusted for multiple comparisons with the use of the Scheffé method. Second, to investigate the association of binary outcomes (eg, subsequent PCI) with BL variables, we used mixed-effect logistic regression with the patient and stent defined as random effect. Third, to investigate the association of continuous outcomes (eg, ISH area) with continuous predictors (eg, BL ESS), we used mixed effects linear regression. BL variables associated with anatomic outcomes on univariable analysis at P level <0.1 were considered for entry in the respective multivariable models, and the final selection of independent predictors was performed with a backward-stepping algorithm (criterion for retention, P<0.1). In the multivariate model where outcome was the dependent variable, baseline parameters were included as independent variables, because all these variables were predictors of outcome on univariable analyses with P<0.1. All statistical tests were 2-tailed, and an α-level of 0.05 was used to determine statistical significance. All statistical analyses were performed with SPSS (version 18.0; SPSS, Inc., Chicago, IL) and Stata software (version 13.0; StataCorp LP, College Station, TX).

The study was approved by the local institutional ethics committee, and each patient gave written informed consent.

Table 2. Medication at Hospital Discharge

Medical Therapy	Available Patients (N=186)
Statin, n (%)	131 (70.4)
Other lipid-lowering medication, n (%)	3 (1.6)
Acetylsalicylic acid, n (%)	166 (89.2)
β-blocker, n (%)	60 (32.3)
Calcium-channel blocker, n (%)	36 (19.4)
Long-acting nitrate, n (%)	26 (14.0)
ACE inhibitor/angiotensin receptor blocker, n (%)	115 (61.8)

ACE indicates angiotensin-converting enzyme.

Table 3. Stent Characteristics

Characteristics	Total (n=246)	Subsequent PCI (n=21)	No Subsequent PCI (n=225)
Procedure type (%)			
ACS culprit lesion	165 (67.0)	19	146
Nonculprit lesion	81 (32.9)	2	79
Vessel (%)			
LAD	161 (65.4)	13	148
RCA	43 (17.5)	5	38
LCX/OM	42 (17.1)	3	39
Stent type (%)			
Bare metal stent (BMS)	100 (40.7)	12	88
Sirolimus-eluting stent (SES)	104 (42.3)	3	101
Paclitaxel-eluting stent (PES)	42 (17.1)	6	36

ACS indicates acute coronary syndrome; LAD, left anterior descending artery; LCX, left circumflex artery; OM, obtuse marginal; PCI, percutaneous coronary intervention; RCA, right coronary artery.

Results

A total of 903 stents were identified at BL in 506 patients (Figure 1). VP at both BL and FU was performed in 374 patients (including 458 stents). Of these, regions with no analyzable or partially analyzable stents (ie, no data for the entire stented region) were excluded, leaving 269 fully analyzable stented regions. Furthermore, we excluded stents implanted before the index BL procedure and stents with ISH at BL (n=20), Zotarolimus-eluting stents (n=2), and stents of unknown type (n=1). In addition, segments with incomplete stent apposition at BL (42 segments) were excluded from this analysis. A total of 246 stents in 186 patients were finally analyzed (161 in the left anterior descending artery, 43 in the left circumflex/obtuse marginal artery, and 42 in the right coronary artery), corresponding to a total of 3659 arterial segments (1.5-mm-long). Fifty-four overlapping stents (833 segments) were included in our analysis. For serial assessment of anatomic changes and hemodynamic effects, each stented region at BL was compared with the corresponding segment at FU.

Patient Demographics and Stent Characteristics

Baseline characteristics of 186 patients are shown in Table 1. A majority of patients had substantial coronary risk factors, but only 13 (7.0%) had a history of past PCI. There were no significant differences of baseline characteristics between available patients in this report and the excluded patients. Medication at hospital discharge are presented in Table 2. Most patients were on routine vasculoprotective therapies. The characteristics of the 246 stents are presented in Table 3. The characteristics of the

Table 4. Baseline and Follow-Up Stent Segments Characteristics in Each Stent Type

Characteristics	Total 246 Stents, 3659 Segments	BMS 100 Stents, 1384 Segments	DES 146 Stents, 2275 Segments	*P* Value BMS vs DES
VA at BL, mm^2	18.48±5.76	20.96±6.17	16.97±4.92	<0.001
LA at BL, mm^2	9.08±2.68	10.19±2.93	8.41±2.26	<0.001
SA at BL, mm^2	9.08±2.68	10.19±2.93	8.41±2.26	<0.001
PA behind the stent at BL, mm^2	9.39±3.84	10.77±4.00	8.55±3.49	<0.001
PB behind the stent at BL, %	49.63±9.11	50.42±8.56	49.15±9.4	<0.001
Minimum ESS at BL, Pa	1.58±1.00	1.42±0.92	1.68±1.03	<0.001
VA at FU, mm^2	18.68±5.53	20.53±6.03	17.55±4.88	<0.001
LA at FU, mm^2	8.08±2.65	7.93±3.05	8.16±2.38	<0.001
SA at FU, mm^2	9.33±2.80	10.54±3.03	8.59±2.37	<0.001
PA behind the stent at FU, mm^2	9.35±3.52	9.99±3.83	8.96±3.25	<0.001
PB behind the stent at FU, %	49.37±8.31	47.90±8.06	50.25±8.34	<0.001
ISH area at FU, mm^2	1.25±1.72	2.62±1.85	0.42±0.94	<0.001
Delta VA, mm^2	0.20±2.74	−0.42±2.98	0.58±2.51	<0.001
Delta LA, mm^2	−1.01±1.94	−2.26±2.04	−0.25±1.41	<0.001
Delta SA, mm^2	0.24±1.36	0.36±1.56	0.17±1.22	<0.001
Delta PA behind the stent, mm^2	−0.04±2.36	−0.78±2.54	0.41±2.13	<0.001
Delta PB behind the stent, %	−0.27±7.64	−2.52±8.30	1.10±6.87	<0.001
%Delta VA, %	2.85±16.54	−0.56±16.89	4.93±16.00	<0.001
%Delta LA, %	−9.76±19.45	−22.26±17.99	−2.15±16.07	<0.001
%Delta SA, %	3.43±14.37	4.40±14.52	2.83±14.25	<0.001
%Delta PA behind the stent, %	6.32±41.70	−0.34±52.64	10.36±32.69	<0.001
%Delta PB behind the stent, %	1.38±20.40	−2.66±25.30	3.84±16.25	<0.001
%ISH area, %	12.39±15.81	25.02±15.89	4.70±9.62	<0.001

Probability values refer to the univariate analysis and are corrected for the clustering of stents within patients. Delta is defined as change in each parameter, which is calculated as respective FU measurement minus BL measurement. BL indicates baseline; BMS, bare-metal stent; DES, drug-eluting stent; ESS, endothelia shear stress; FU, follow-up; ISH, in-stent hyperplasia; LA, lumen area; PA, plaque area; PB, plaque burden; SA, stent area; VA, vessel area.

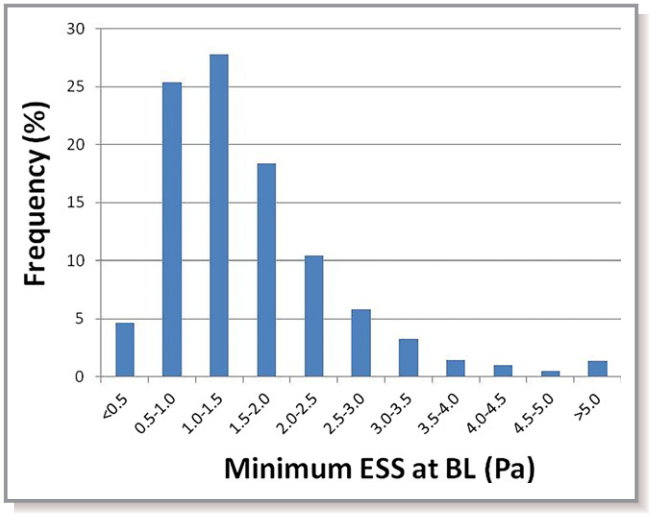

Figure 2. Distribution of post-PCI minimum ESS at BL. Distribution of post-PCI minimum ESS in 1.5-mm segments at BL (n=3659). The highest distribution range was 1.0 to 1.5 Pa (27.8%). BL indicates baseline; ESS, endothelial shear stress; PCI, percutaneous coronary intervention.

3659 stent segments at BL and FU are presented in Table 4. The mean BL ESS magnitude within the stented area after stent deployment was 1.57±1.00 Pa (median, 1.34 Pa; IQR, 0.92–1.95). The frequency distribution of post-PCI BL ESS magnitude within the stented region is shown in Figure 2, demonstrating that ESS most commonly ranged between 1.0 and 1.5 Pa (27.8%).

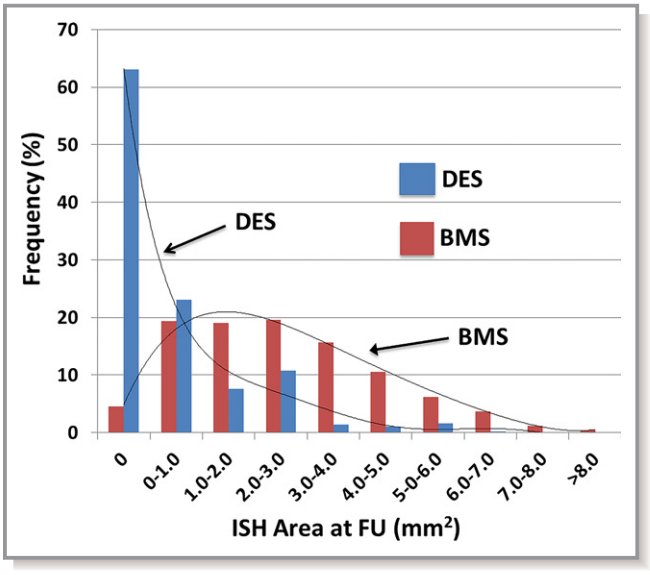

Figure 3. Distribution of ISH Area in BMS and DES. Distribution of ISH area in 1.5-mm segments at FU compared with each stent type. ISH area at FU was significantly larger in BMS than in DES (P<0.001). BMS indicates bare-metal stent; DES, drug-eluting stent; FU, follow-up; ISH, in-stent hyperplasia.

Table 5. Relationship Between Baseline Stent Characteristics and ISH Outcomes in BMS (1.5-mm Segments; n=1384): Univariable Analyses

Outcome	Baseline Predictors	Beta (95% CI)	*P* Value
ISH area, mm^2	Vessel area (per 1-mm^2 increase)	0.13 (0.11–0.16)	<0.001
	Stent area (per 1-mm^2 increase)	0.18 (0.13–0.23)	<0.001
	Plaque area behind the stent (per 1-mm^2 increase)	0.16 (0.13–0.19)	<0.001
	Plaque burden behind the stent (per 10% increase)	0.46 (0.34–0.58)	<0.001
	ESS (per 1-Pa decrease)	0.29 (0.17–0.41)	<0.001
%ISH area (%)	Vessel area (per 1-mm^2 increase)	0.83 (0.63–1.02)	<0.001
	Stent area (per 1-mm^2 increase)	0.41 (−0.02–0.85)	0.064
	Plaque area behind the stent (per 1-mm^2 increase)	1.22 (0.96–1.48)	<0.001
	Plaque burden behind the stent (per 10% increase)	4.94 (3.90–8.98)	<0.001
	ESS (per 1-Pa decrease)	1.32 (0.33–2.32	0.009

BMS indicates bare-metal stent; ESS, endothelial shear stress; ISH, in-stent hyperplasia.

Anatomical Outcomes for Each Stent Type

Among the 246 stents, including overlap stents, 100 (40.7%) were BMS and 142 (59.3%) were DES (Table 3). Analyzing the stented segments as consecutive 1.5-mm segments yielded 1384 segments for BMS and 2275 for DES. Anatomical characteristics of stented segments are presented in Table 4. The frequency distribution of ISH area by individual stent type is shown in Figure 3. The highest proportion of ISH area at FU was between 2.0 and 3.0 mm^2 for BMS (20.1%) and between 0 and 1.0 mm^2 for DES (63.0%). Because there was very little ISH in the DES regions, we were unable to evaluate the impact of local ESS within the stented region on ISH in these stents; our analyses of the effect of baseline ESS within the stented region and subsequent neointimal ISH were therefore limited to the BMS regions.

Effect of Baseline In-Stent Characteristics on Neointimal ISH

Large stent area and large plaque burden behind the stent were independently associated with the magnitude of ISH

Table 6. Independent Baseline Predictors of ISH Outcomes in BMS (1.5-mm Segments; n=1384): Multivariable Analysis

Outcome	Baseline Predictors	Beta (95% CI)	*P* Value
ISH area, mm^2	Stent area (per 1-mm^2 increase)	0.21 (0.15–0.27)	<0.001
	Plaque burden behind the stent (per 10% increase)	0.59 (0.47–0.71)	<0.001
	ESS (per 1-Pa decrease)	0.12 (−0.01–0.25)	0.072
%ISH area (%)	Vessel area (per 1-mm^2 increase)	0.27 (0.02–0.52)	0.037
	Plaque burden behind the stent (per 10% increase)	4.50 (3.21–5.78)	<0.001
	ESS (per 1-Pa decrease)	1.47 (0.38–2.56)	0.008

In the multivariable model where ISH area is the dependent variable, vessel area, stent area, plaque area behind the stent, plaque burden behind the stent, and ESS at baseline were included as independent variables, because all these variables were predictors of ISH area on univariable analyses with $P<0.1$. In this multivariable model, large stent area and large plaque burden behind the stent were independently associated with ISH area. In the multivariable model where % ISH area is the dependent variable, vessel area, stent area, plaque area behind the stent, plaque burden behind the stent, and ESS at baseline were included as independent variables. In this multivariable model, large vessel area, large plaque burden behind the stent, and low ESS were independently associated with % ISH area. ESS indicates endothelial shear stress; ISH, in-stent hyperplasia.

area (Tables 5 and 6). Large vessel area, large plaque burden behind the stent, and low ESS at BL were independent predictors of %ISH area.

Effect of ESS on Neointimal ISH in Overlapping and Nonoverlapping Stent Segments

At BL, 9 overlapping BMS (9.0%) and 45 overlapping DES (18.3%) were documented, corresponding to 122 and 711 segments for each stent type, respectively. There were no significant differences in ISH area and %ISH area between overlapping and nonoverlapping regions in stent types. In stented regions with overlap, low ESS at BL was not associated with ISH outcomes in univariate analysis for BMS (Table 7). In stented regions without overlap, low ESS at BL was independently associated with the ISH area and %ISH area in BMS (Table 8).

ESS and ISH in Stents Implanted at ACS Culprit Lesions Versus Nonculprit Lesions

At BL, 165 stents (67.0%) were implanted at an ACS culprit lesion and 81 stents (32.9%) at nonculprit lesions. In ACS culprit lesion stents, 88 (53.3%) were BMS and 77 (46.7%) were DES. The comparison of stented regions involving the ACS culprit lesion and those involving the nonculprit lesion at BL and FU is presented in Table 9. The magnitude of ESS at BL was significantly lower in stented segments involving the ACS culprit lesion compared with stents at nonculprit lesions (1.49±0.89 vs 1.73±1.15 Pa; $P<0.001$). Furthermore, ISH area and %ISH area at FU were significantly larger in stented segments involving the ACS culprit lesion than in stents at nonculprit lesions.

Baseline Characteristics of Stents With ISR Requiring Subsequent PCI at FU Versus Stents Without ISR

At FU, subsequent PCI for a significantly worsened luminal obstruction was performed in 21 stents (8.5%; n=242 segments). Of these, 12 stents (n=134 segments) were BMS. The comparison of stented regions treated with or without subsequent PCI is shown in Table 10. The magnitude of ESS at BL within the stented regions was not significantly different between the subsequent PCI group and the no subsequent PCI group (1.54±1.00 vs 1.58±1.00 Pa; $P=0.754$). Figure 4 shows the distribution of ISH area at FU in the subsequent PCI group versus the no subsequent PCI group. ISH area was significantly higher in the subsequent PCI group (255±1.89 mm^2; median, 2.17 [IQR, 1.10–3.70]) than in the no subsequent PCI group (1.16±1.67 mm^2; median, 0.24 [IQR, 0–1.85]; $P<0.001$).

Baseline Predictors of ISR Requiring Subsequent PCI at FU

In univariate analyses, small stent area (per 1-mm^2 decrease), large plaque area behind the stent (per 1-mm^2 increase), and large plaque burden behind the stent (per 10% increase) were BL predictors of subsequent PCI. In multivariable analysis, independent predictors of subsequent PCI for ISR were small stent area (per 1-mm^2 decrease) and large plaque burden behind the stent (per 10% increase; odds ratio [OR], 1.39; 95% CI, 1.01–1.89; $P=0.040$ and OR, 2.65; 95% CI, 1.56–4.48; $P<0.001$, respectively; Table 11). There was no significant relationship between ESS within the stented region at BL and subsequent PCI.

Discussion

This study demonstrates, for the first time, the effect of in-stent ESS on subsequent ISH in a large patient population. The main findings of this report are that: (1) ISH after BMS implantation is independently associated with the preceding low ESS within the stented region, regardless of whether the stented region consists of overlapping or nonoverlapping segments, and (2) the magnitude of ESS within the stent at BL is not associated with ISR requiring subsequent PCI at FU.

Table 7. Relationship Between Baseline Stent Characteristics of Overlapping and Nonoverlapping Stents and ISH Outcomes in BMS: Univariable Analyses

	Outcome	Baseline Predictors	Beta (95% CI)	*P* Value
Overlapping stents	ISH area, mm^2	Vessel area (per 1-mm^2 increase)	0.12 (0.097–0.14)	<0.001
		Stent area (per 1-mm^2 increase)	0.16 (0.11–0.22)	<0.001
		Plaque area behind the stent (per 1-mm^2 increase)	0.15 (0.11–0.18)	<0.001
		Plaque burden behind the stent (per 10% increase)	0.39 (0.25–0.52)	<0.001
		ESS (per 1-Pa decrease)	0.36 (0.22–0.50)	<0.001
	%ISH area (%)	Vessel area (per 1-mm^2 increase)	0.65 (0.44–0.85)	<0.001
		Stent area (per 1-mm^2 increase)	0.26 (−0.18 to 0.71)	0.24
		Plaque area behind the stent (per 1-mm^2 increase)	0.98 (0.71–1.25)	<0.001
		Plaque burden behind the stent (per 10% increase)	3.92 (2.79–5.06)	<0.001
		ESS (per 1-Pa decrease)	1.57 (0.39–2.76)	0.009
Nonoverlapping stents	ISH area, mm^2	Vessel area (per 1-mm^2 increase)	0.12 (0.097–0.14)	<0.001
		Stent area (per 1-mm^2 increase)	0.16 (0.11–0.22)	<0.001
		Plaque area behind the stent (per 1-mm^2 increase)	0.15 (0.11–0.18)	<0.001
		Plaque burden behind the stent (per 10% increase)	0.39 (0.25–0.52)	<0.001
		ESS (per 1-Pa decrease)	0.36 (0.22–0.50)	<0.001
	%ISH area (%)	Vessel area (per 1-mm^2 increase)	0.65 (0.44–0.85)	<0.001
		Stent area (per 1-mm^2 increase)	0.26 (−0.18 to 0.71)	0.24
		Plaque area behind the stent (per 1-mm^2 increase)	0.98 (0.71–1.25)	<0.001
		Plaque burden behind the stent (per 10% increase)	3.92 (2.79–5.06)	<0.001
		ESS (per 1-Pa decrease)	1.57 (0.39–2.76)	0.009

BMS indicates bare-metal stent; ESS, endothelial shear stress; ISH, in-stent hyperplasia.

Stent Deployment, Vascular Flow Alterations, and ISH

The effects of arterial flow alterations in stent deployment involve multiscale phenomena. Bulk flow changes attributed to the cardiac ejection create time-dependent flow and pressure drops across vascular segments that change as a function of vascular impedance and dimensions. Geometrical irregularities in the vasculature, such as curvature in highly tortuous vessel and the presence of lesions and stents, also cause ESS variations. Physiological ESS inhibits smooth muscle cell (SMC) proliferation and migration either directly or through endothelial cells,[21] whereas low ESS promotes the activation, proliferation, and migration of SMCs by increasing expression of platelet-derived growth factors, endothelin-1, and vascular-endothelial growth factors. Therefore, native lesions that are exposed to low ESS (ESS <1.0 Pa) exhibit augmented plaque progression.[15] Although the impact of ESS on vascular response within a stent has been studied before,[8,11,13,18,22] data still remain inconclusive.

At the stent strut level, arterial flow introduces micro-scale near-wall flow alterations, creating recirculating zones local to the stent struts. The extent and magnitude of these flow disturbances are a function of stent dimensions, strut configuration, strut apposition relative to the arterial wall[23] and stent overlap.[24] These local flow alterations mediate biological responses through increased thrombogenicity[25] and impaired rate of vascular repair,[26] with mechanisms different than macro-scale effects.[27] In the case of DES, the impact of arterial drug distribution is further modulated with variable convective transport environments.[28]

In this work, we show the impact of macro-scale flow alterations attributed to stent deployment on ISH in patient-specific scenarios; we did not have appropriate data to address micro-scale effects. Similar to an earlier study,[18] our methods included defining the arterial geometry by using IVUS and angiography and modeling the stent as a distinct region in the arterial wall bounded by the stent struts. By isolating the macro-scale events, we were then able to investigate their predictive role in ISH and ISR. Local post-PCI ESS independently predicts %ISH area in BMS, but not ISR at FU. The absolute ISH area is dependent on stent size, especially in BMS, and this study included various stent sizes, as a reflection of its large-scale nature. However, when we

Table 8. Independent Baseline Predictors of ISH Outcomes in Overlap Stents and Nonoverlap Stents for BMS: Multivariable Analysis

	Outcome	Baseline Predictors	Beta (95% CI)	*P* Value
ISH area, mm^2	Overlap stent	Vessel area (per 1-mm^2 increase)	0.31 (0.25–0.36)	<0.001
	Nonoverlap stent	Vessel area (per 1-mm^2 increase)	0.086 (0.054–0.12)	<0.001
		Plaque burden behind the stent (per 10% increase)	0.22 (0.050–0.39)	0.011
		ESS (per 1-Pa decrease)	0.25 (0.088–0.41)	0.003
%ISH area (%)	Overlap stent	Vessel area (per 1-mm^2 increase)	1.67 (0.79–2.56)	<0.001
		Plaque burden behind the stent (per 10% increase)	5.61 (2.34–8.88)	0.001
	Nonoverlap stent	Plaque burden behind the stent (per 10% increase)	4.60 (3.44–5.76)	<0.001
		ESS (per 1-Pa decrease)	2.69 (1.50–3.88)	<0.001

In the multivariable model where ISH area with overlap stent is the dependent variable, vessel area, stent area, plaque area behind the stent, and plaque burden behind the stent at baseline were included as independent variables, because all these variables were predictors of ISH on univariable analyses with $P<0.1$. In this multivariable model, large vessel area was independently associated with ISH area with overlap. In the multivariable model where ISH area without overlap stent is the dependent variable, vessel area, stent area, plaque area behind the stent, plaque burden behind the stent, and ESS at baseline were included as independent variables. In this multivariable model, large vessel area, plaque burden behind the stent and low ESS were independently associated with ISH area without overlap. In the multivariable model where %ISH area with overlap stent is the dependent variable, vessel area, plaque area behind the stent, and plaque burden behind the stent at baseline were included as independent variables, because all these variables were predictors of %ISH on univariable analyses with $P<0.1$. In this multivariable model, large vessel area and large plaque behind the stent were independently associated with %ISH area with overlap. In the multivariable model where %ISH area without overlap stent is the dependent variable, vessel area, plaque area behind the stent, plaque burden behind the stent, and ESS at baseline were included as independent variables. In this multivariable model, plaque burden behind the stent and low ESS were independently associated with %ISH area without overlap. ESS indicates endothelial shear stress; ISH, in-stent hyperplasia.

normalized ISH area to stent area (ie, %ISH area), we identified the relationship between ESS and local vascular responses, which was similar to previous smaller-scale clinical studies.[8,9,13] Our study showed that only 27.2% of all stents were fully analyzable at BL and FU. The major cause of exclusion was that VP data were not available for the entire stent (Figure 1). However, there were no significant differences in baseline patient characteristics between included and excluded stents, and a selection bias is very unlikely to account for our results.

Impact of Eluted Compound on ISH

DES has been shown to markedly reduce the occurrence of severe ISH.[29,30] Local delivery of antineoplastic agents from the stent strut to the arterial tissue inhibits ISH growth and leads to clinical benefit. Flow environments and arterial patterns affect drug delivery and drug-specific effects.[28,31,32] Nevertheless, DES is not immune to ISR. In fact, a previous study in a large cohort of patients with angiographic surveillance reported that ISR rate remains higher than10%.[33] A recent study retrospectively analyzed IVUS data in 298 ISR to compare the mechanisms of ISR between BMS and DES,[34] and found that both neointimal hyperplasia (NIH) and stent under expansion were mechanisms of ISR. In our study, although the lack of an ISH response within the DES group precluded further evaluation of the role of flow in ISH outcomes in those regions, it remains possible that NIH is large at low ESS areas within DES.

Impact of Stent Overlap on ISH

Stent overlap occurs in more than 30% of cases, and less-favorable outcomes are consistently reported in this setting with both BMS[4,35] and DES.[14] Studies have observed more neutrophils, eosinophils, and fibrin deposition, suggestive of more-intense inflammation and therefore of an underlying flow-related vascular response mechanism. In this study, we found ESS to independently predict ISH area in nonoverlapped segments, but, interestingly, not in the case of stent overlap. This could either be a result of the small group size of overlapping stents (n=54 stents) or suggest that another scale of flow could dominate in areas of stent overlap, in particular, those micro-scale flow alterations near stent struts. When multiple stents are deployed, the inner stent will augment further those strut-induced flow alterations[25] and will increase both the area of arterial wall exposed to prorestenotic flow[24] and the magnitude and amplitude of ESS variations across the vessel. The limited resolution of our clinical imaging did not allow for the reconstruction and coregistration of multiscale flow models and the study of associated in vivo biological responses.

Impact of the BL Clinical Presentation on ISH

The pathophysiology and prognosis of ACS-associated plaques is different than non-ACS-associated plaques, with ACS plaques exhibiting a more-pronounced inflammatory response than stable angina lesions. Our study showed that the magnitude of ESS within the stented region at BL was lower in the case of ACS, and ISH at FU was also larger.

Table 9. Comparison of Stent Segments at ACS Culprit Lesion and Nonculprit Lesion

Characteristics	ACS Culprit Lesion (165 Stents, 2360 Segments)	Nonculprit Lesion (81 Stents, 1299 Segments)	*P* Value
VA at BL, mm^2	19.79±5.76	16.09±4.92	<0.001
LA at BL, mm^2	9.56±2.75	8.21±2.29	<0.001
SA at BL, mm^2	9.56±2.75	8.21±2.29	<0.001
PA behind the stent at BL, mm^2	10.23±3.82	7.88±3.39	<0.001
PB behind the stent at BL, %	50.74±8.72	47.63±9.45	<0.001
Minimum ESS at BL, Pa	1.49±0.89	1.73±1.15	0.001
VA at FU, mm^2	19.73±5.68	16.76±4.69	<0.001
LA at FU, mm^2	8.29±2.90	7.68±2.09	0.165
SA at FU, mm^2	9.91±2.89	8.28±2.30	<0.001
PA behind the stent at FU, mm^2	9.82±3.61	8.49±3.16	<0.001
PB behind the stent at FU, %	49.15±8.04	49.74±8.78	<0.001
ISH area at FU, mm^2	1.62±1.85	0.59±1.21	<0.001
Delta VA, mm^2	−0.06±2.94	0.68±2.28	<0.001
Delta LA, mm^2	−1.27±2.13	−0.53±1.43	<0.001
Delta SA, mm^2	0.34±1.49	0.07±1.06	0.459
Delta PA behind the stent, mm^2	−0.40±2.39	0.61±2.18	<0.001
Delta PB behind the stent, %	−1.59±7.15	2.12±7.93	<0.001
%Delta VA, %	1.13±17.04	5.98±15.14	<0.001
%Delta LA, %	−12.39±20.63	−4.99±16.04	<0.001
%Delta SA, %	4.43±15.15	1.59±12.63	0.427
%Delta PA behind the stent, %	1.68±43.56	14.74±36.63	<0.001
%Delta PB behind the stent, %	−1.48±19.97	6.59±20.14	<0.001
%ISH area, %	15.73±16.83	6.31±11.51	<0.001

Probability values refer to the univariate analysis and are corrected for the clustering of stents within patients. ACS indicates acute coronary syndrome; BL, baseline; ESS, endothelia shear stress; FU, follow-up; ISH, in-stent hyperplasia; LA, lumen area; PA, plaque area; PB, plaque burden; SA, stent area; VA, vessel area.

Table 10. Comparison of Stent Segments Treated by Subsequent PCI and No Subsequent PCI

Characteristics	Subsequent PCI (21 Stents, 242 Segments)	No Subsequent PCI (225 Stents, 3417 Segments)	*P* Value
VA at BL, mm^2	16.59±5.60	18.61±5.75	0.572
LA at BL, mm^2	8.28±2.20	9.14±2.70	<0.001
SA at BL, mm^2	8.28±2.20	9.14±2.70	<0.001
PA behind the stent at BL, mm^2	8.3±3.75	9.47±3.84	0.006
PB behind the stent at BL, %	48.42±7.76	49.72±9.19	<0.001
Minimum ESS at BL, Pa	1.54±1.00	1.58±1.00	0.754
VA at FU, mm^2	17.14±5.36	18.79±5.53	0.537
LA at FU, mm^2	5.98±1.89	8.22±2.64	<0.001
SA at FU, mm^2	8.53±2.45	9.38±2.82	0.001
PA behind the stent at FU, mm^2	8.61±3.61	9.40±3.51	0.280
PB behind the stent at FU, %	49.30±8.41	49.37±8.31	0.002
ISH area at FU, mm^2	2.55±1.89	1.16±1.67	<0.001
Delta VA, mm^2	0.55±2.62	0.18±2.75	0.145
Delta LA, mm^2	−2.30±1.85	−0.92±1.92	<0.001
Delta SA, mm^2	0.24±1.12	0.24±1.37	0.671
Delta PA behind the stent, mm^2	0.31±2.60	−0.07±2.34	0.036
Delta PB behind the stent, %	0.88±9.29	−0.35±7.51	0.187
%Delta VA, %	6.07±19.93	2.63±16.27	0.280
%Delta LA, %	−26.29±18.62	−8.58±18.97	<0.001
%Delta SA, %	3.13±13.04	3.44±14.46	0.899
%Delta PA behind the stent, %	14.02±55.47	5.77±40.50	0.174
%Delta PB behind the stent, %	3.91±23.93	1.20±20.12	0.192
%ISH area, %	28.18±16.68	11.25±15.14	<0.001

Probability values refer to the univariate analysis and are corrected for the clustering of stents within patients. BL indicates baseline; ESS, endothelia shear stress; FU, follow-up; ISH, in-stent hyperplasia; LA, lumen area; PA, plaque area; PB, plaque burden; PCI, percutaneous coronary intervention; SA, stent area; VA, vessel area.

Stents in ACS culprit lesions also exhibited a higher degree of luminal narrowing from BL to FU, despite plaque regression behind the stent. These findings might be affected by the low ESS within the stented region at BL and the high proportion of BMS implanted at ACS culprit lesions. Previous reports have demonstrated that angiographic restenosis is more frequent in patients with ACS than with stable angina, which is consistent with our results.[36]

Impact of ESS on ISR Requiring Repeat PCI

Our study did not demonstrate a significant relationship between low ESS within the BMS stented region at BL and occurrence of a subsequent clinically indicated PCI at FU. Low ESS was an independent predictor of ISH at FU, and the ISH area

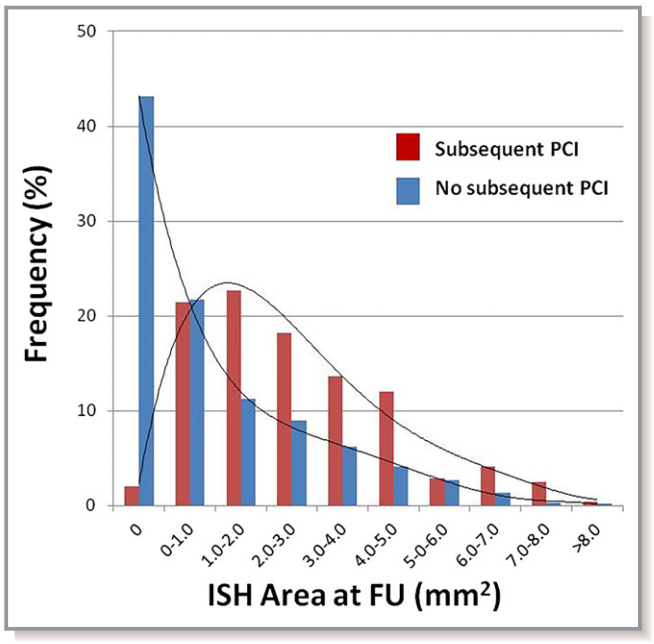

Figure 4. Distribution of ISH area with subsequent PCI or not. Distribution of ISH area in 1.5-mm segments at FU compared with subsequent PCI group and no subsequent PCI group. There were 242 segments (BMS, 134 segments [55.3%]; DES, 108 segments [44.6%]) in subsequent PCI group and 3417 segments (BMS, 1250 segments [36.6%]; DES, 2167 segments [63.4%]) in no subsequent PCI group. ISH area at FU was significantly larger in subsequent PCI group than in no subsequent PCI group ($P<0.001$). BMS indicates bare-metal stent; DES, drug-eluting stent; FU, follow-up; ISH, in-stent hyperplasia; PCI, percutaneous coronary intervention.

at FU was significantly larger in stents with FU ISR PCI than in those without ISR. Given that late lumen loss correlates with neointimal tissue proliferation, the magnitude of ISH conceptually contributes to a clinically dictated revascularization. Our results indicate, however, that though low ESS was associated with ISH during this short-term FU, there was not sufficient ISH that would cause ISR and warrant repeat revascularization.

Study Limitations

Our study had several limitations. We did not collect information concerning the specific type of BMS utilized. Although stent design and configuration are important for the hemodynamic environment, our definition of flow in this study was a macroscopic measure of flow in the stented region and did not reflect the microscopic flow patterns associated with specific stent geometries. We were also limited to BMS cases only in ISH assessment because there was very little ISH observed in DES. Our study is also limited by the small number of clinical events that occurred within the short FU period. Many of these clinical events were asymptomatic, consisting of significant in-stent lumen narrowing identified during routine FU cardiac catheterization and, accordingly, treated with a PCI.

Table 11. Baseline Anatomic Predictors of Subsequent PCI

	Baseline Predictor	Odds Ratio (95% CI)	*P* Value
Univariable analysis	Vessel wall area (per 1-mm^2 increase)	1.04 (0.94–1.16)	0.448
	Stent area (per 1-mm^2 decrease)	1.56 (1.15–2.11)	0.004
	Plaque area behind the stent (per 1-mm^2 increase)	1.30 (1.11–1.53)	0.001
	Plaque burden behind the stent (per 10% increase)	3.00 (1.78–5.07)	<0.001
	ESS (per 1-Pa decrease)	0.79 (0.45–1.39)	0.416
Multivariable analysis	Stent area (per 1-mm^2 decrease)	1.39 (1.01–1.89)	0.040
	Plaque burden behind the stent (per 10% increase)	2.65 (1.56–4.48)	<0.001

In the multivariable model where subsequent PCI is the dependent variable, stent area, plaque area behind the stent, and plaque burden behind the stent at baseline were included as independent variables, because all these variables were predictors of subsequent PCI on univariable analyses with $P<0.1$. In this multivariable model, small stent area and large plaque burden behind the stent were independently associated with subsequent PCI. ESS indicates endothelial shear stress; PCI, percutaneous coronary intervention.

Although in-stent thrombosis occurred in a few cases, it was not feasible to obtain VP data in those emergency clinical situations. Therefore, we were not able to investigate the relationship between ESS within the stent and late or very late stent thrombosis, which is an important component in the management of patients with DES.

Conclusions

ISH after stent implantation relates to preceding low ESS within the stent. ISH is strongly inhibited by DES. ESS is not associated with ISR requiring subsequent PCI at FU. Although low ESS is independently associated with ISH, it does not predict ISH of sufficiently large magnitude to cause clinically evident lumen obstruction. ESS is an important determinant of ISH after stent implantation, but pronounced ISH during this short FU is likely attributed to factors other than local ESS within the stented region.

Sources of Funding

The PREDICTION Study was funded by Boston Scientific Company. We gratefully acknowledge the support from the George D. Behrakis Cardiovascular Research Program, the Hellenic Cardiological Society, and the Schaubert Family.

Disclosures

None.

References

1. Hoffmann R, Mintz GS, Dussaillant GR, Popma JJ, Pichard AD, Satler LF, Kent KM, Griffin J, Leon MB. Patterns and mechanisms of in-stent restenosis. A serial intravascular ultrasound study. *Circulation*. 1996;94:1247–1254.
2. Moses JW, Leon MB, Popma JJ, Fitzgerald PJ, Holmes DR, O'Shaughnessy C, Caputo RP, Kereiakes DJ, Williams DO, Teirstein PS, Jaeger JL, Kuntz RE; Investigators S. Sirolimus-eluting stents versus standard stents in patients with stenosis in a native coronary artery. *N Engl J Med*. 2003;349:1315–1323.
3. Morice MC, Colombo A, Meier B, Serruys P, Tamburino C, Guagliumi G, Sousa E, Stoll HP; Investigators RT. Sirolimus- vs paclitaxel-eluting stents in de novo coronary artery lesions: the REALITY trial: a randomized controlled trial. *JAMA*. 2006;295:895–904.
4. Kornowski R, Hong MK, Tio FO, Bramwell O, Wu H, Leon MB. In-stent restenosis: contributions of inflammatory responses and arterial injury to neointimal hyperplasia. *J Am Coll Cardiol*. 1998;31:224–230.
5. van Beusekom HM, Whelan DM, Hofma SH, Krabbendam SC, van Hinsbergh VW, Verdouw PD, van der Giessen WJ. Long-term endothelial dysfunction is more pronounced after stenting than after balloon angioplasty in porcine coronary arteries. *J Am Coll Cardiol*. 1998;32:1109–1117.
6. Koskinas KC, Chatzizisis YS, Antoniadis AP, Giannoglou GD. Role of endothelial shear stress in stent restenosis and thrombosis: pathophysiologic mechanisms and implications for clinical translation. *J Am Coll Cardiol*. 2012;59:1337–1349.
7. Wentzel JJ, Gijsen FJ, Schuurbiers JC, van der Steen AF, Serruys PW. The influence of shear stress on in-stent restenosis and thrombosis. *EuroIntervention*. 2008;4 suppl C:C27–C32.
8. Wentzel JJ, Krams R, Schuurbiers JCH, Oomen JA, Kloet J, van der Giessen WJ, Serruys PW, Slager CJ. Relationship between neointimal thickness and shear stress after Wallstent implantation in human coronary arteries. *Circulation*. 2001;103:1740–1745.
9. Sanmartin M, Goicolea J, Garcia C, Garcia J, Crespo A, Rodriguez J, Goicolea JM. Influence of shear stress on in-stent restenosis: in vivo study using 3D reconstruction and computational fluid dynamics. *Rev Esp Cardiol*. 2006;59:20–27.
10. Papafaklis MI, Bourantas CV, Theodorakis PE, Katsouras CS, Fotiadis DI, Michalis LK. Relationship of shear stress with in-stent restenosis: bare metal stenting and the effect of brachytherapy. *Int J Cardiol*. 2009;134:25–32.
11. Gijsen FJ, Oortman RM, Wentzel JJ, Schuurbiers JC, Tanabe K, Degertekin M, Ligthart JM, Thury A, de Feyter PJ, Serruys PW, Slager CJ. Usefulness of shear stress pattern in predicting neointima distribution in sirolimus-eluting stents in coronary arteries. *Am J Cardiol*. 2003;92:1325–1328.
12. Suzuki N, Nanda H, Angiolillo DJ, Bezerra H, Sabate M, Jimenez-Quevedo P, Alfonso F, Macaya C, Bass TA, Ilegbusi OJ, Costa MA. Assessment of potential relationship between wall shear stress and arterial wall response after bare metal stent and sirolimus-eluting stent implantation in patients with diabetes mellitus. *Int J Cardiovasc Imaging*. 2008;24:357–364.
13. Papafaklis MI, Bourantas CV, Theodorakis PE, Katsouras CS, Naka KK, Fotiadis DI, Michalis LK. The effect of shear stress on neointimal response following sirolimus- and paclitaxel-eluting stent implantation compared with bare-metal stents in humans. *JACC Cardiovasc Interv*. 2010;3:1181–1189.
14. Raber L, Juni P, Loffel L, Wandel S, Cook S, Wenaweser P, Togni M, Vogel R, Seiler C, Eberli F, Luscher T, Meier B, Windecker S. Impact of stent overlap on angiographic and long-term clinical outcome in patients undergoing drug-eluting stent implantation. *J Am Coll Cardiol*. 2010;55:1178–1188.
15. Stone PH, Saito S, Takahashi S, Makita Y, Nakamura S, Kawasaki T, Takahashi A, Katsuki T, Nakamura S, Namiki A, Hirohata A, Matsumura T, Yamazaki S, Yokoi H, Tanaka S, Otsuji S, Yoshimachi F, Honye J, Harwood D, Reitman M, Coskun AU, Papafaklis MI, Feldman CL; Investigators P. Prediction of progression of coronary artery disease and clinical outcomes using vascular profiling of endothelial shear stress and arterial plaque characteristics: the PREDICTION Study. *Circulation*. 2012;126:172–181.
16. Feldman CL, Ilegbusi OJ, Hu Z, Nesto R, Waxman S, Stone PH. Determination of in vivo velocity and endothelial shear stress patterns with phasic flow in human coronary arteries: a methodology to predict progression of coronary atherosclerosis. *Am Heart J*. 2002;143:931–939.
17. Coskun AU, Yeghiazarians Y, Kinlay S, Clark ME, Ilegbusi OJ, Wahle A, Sonka M, Popma JJ, Kuntz RE, Feldman CL, Stone PH. Reproducibility of coronary lumen, plaque, and vessel wall reconstruction and of endothelial shear stress measurements in vivo in humans. *Catheter Cardiovasc Interv*. 2003;60:67–78.
18. Stone PH, Coskun AU, Kinlay S, Clark ME, Sonka M, Wahle A, Ilegbusi OJ, Yeghiazarians Y, Popma JJ, Orav J, Kuntz RE, Feldman CL. Effect of endothelial shear stress on the progression of coronary artery disease, vascular remodeling, and in-stent restenosis in humans: in vivo 6-month follow-up study. *Circulation*. 2003;108:438–444.
19. Chatzizisis YS, Jonas M, Coskun AU, Beigel R, Stone BV, Maynard C, Gerrity RG, Daley W, Rogers C, Edelman ER, Feldman CL, Stone PH. Prediction of the localization of high-risk coronary atherosclerotic plaques on the basis of low endothelial shear stress: an intravascular ultrasound and histopathology natural history study. *Circulation*. 2008;117:993–1002.
20. Sakamoto S, Takahashi S, Coskun AU, Papafaklis MI, Takahashi A, Saito S, Stone PH, Feldman CL. Relation of distribution of coronary blood flow volume to coronary artery dominance. *Am J Cardiol*. 2013;111:1420–1424.
21. Ueba H, Kawakami M, Yaginuma T. Shear stress as an inhibitor of vascular smooth muscle cell proliferation. Role of transforming growth factor-beta 1 and tissue-type plasminogen activator. *Arterioscler Thromb Vasc Biol*. 1997;17:1512–1516.
22. Bourantas CV, Papafaklis MI, Kotsia A, Farooq V, Muramatsu T, Gomez-Lara J, Zhang YJ, Iqbal J, Kalatzis FG, Naka KK, Fotiadis DI, Dorange C, Wang J, Rapoza R, Garcia-Garcia HM, Onuma Y, Michalis LK, Serruys PW. Effect of the endothelial shear stress patterns on neointimal proliferation following drug-eluting bioresorbable vascular scaffold implantation: an optical coherence tomography study. *JACC Cardiovasc Interv*. 2014;7:315–324.
23. O'Brien CC, Finch CH, Barber TJ, Martens P, Simmons A. Analysis of drug distribution from a simulated drug-eluting stent strut using an in vitro framework. *Ann Biomed Eng*. 2012;40:2687–2696.
24. Rikhtegar F, Wyss C, Stok KS, Poulikakos D, Muller R, Kurtcuoglu V. Hemodynamics in coronary arteries with overlapping stents. *J Biomech*. 2014;47:505–511.
25. Kolandaivelu K, Swaminathan R, Gibson WJ, Kolachalama VB, Nguyen-Ehrenreich KL, Giddings VL, Coleman L, Wong GK, Edelman ER. Stent thrombogenicity early in high-risk interventional settings is driven by stent design and deployment and protected by polymer-drug coatings. *Circulation*. 2011;123:1400–1409.
26. Foin N, Gutierrez-Chico JL, Nakatani S, Torii R, Bourantas CV, Sen S, Nijjer S, Petraco R, Kousera C, Ghione M, Onuma Y, Garcia-Garcia HM, Francis DP, Wong P, Di Mario C, Davies JE, Serruys PW. Incomplete stent apposition causes high shear flow disturbances and delay in neointimal coverage as a function of strut to wall detachment distance: implications for the management of incomplete stent apposition. *Circ Cardiovasc Interv*. 2014;7:180–189.
27. Jimenez JM, Prasad V, Yu MD, Kampmeyer CP, Kaakour AH, Wang PJ, Maloney SF, Wright N, Johnston I, Jiang YZ, Davies PF. Macro- and microscale variables regulate stent haemodynamics, fibrin deposition and thrombomodulin expression. *J R Soc Interface*. 2014;11:20131079.
28. Balakrishnan B, Tzafriri AR, Seifert P, Groothuis A, Rogers C, Edelman ER. Strut position, blood flow, and drug deposition: implications for single and overlapping drug-eluting stents. *Circulation*. 2005;111:2958–2965.
29. Stefanini GG, Holmes DR Jr. Drug-eluting coronary-artery stents. *N Engl J Med*. 2013;368:254–265.
30. Sousa JE, Serruys PW, Costa MA. New frontiers in cardiology: drug-eluting stents: Part I. *Circulation*. 2003;107:2274–2279.
31. O'Brien CC, Kolachalama VB, Barber TJ, Simmons A, Edelman ER. Impact of flow pulsatility on arterial drug distribution in stent-based therapy. *J Control Release*. 2013;168:115–124.
32. Tzafriri AR, Vukmirovic N, Kolachalama VB, Astafieva I, Edelman ER. Lesion complexity determines arterial drug distribution after local drug delivery. *J Control Release*. 2010;142:332–338.
33. Cassese S, Byrne RA, Tada T, Pinieck S, Joner M, Ibrahim T, King LA, Fusaro M, Laugwitz KL, Kastrati A. Incidence and predictors of restenosis after coronary stenting in 10004 patients with surveillance angiography. *Heart*. 2014;100:153–159.
34. Goto K, Zhao Z, Matsumura M, Dohi T, Kobayashi N, Kirtane AJ, Rabbani LE, Collins MB, Parikh MA, Kodali SK, Leon MB, Moses JW, Mintz GS, Maehara A. Mechanisms and patterns of intravascular ultrasound in-stent restenosis among bare metal stents and first- and second-generation drug-eluting stents. *Am J Cardiol*. 2015;116:1351–1357.
35. Ellis SG, Savage M, Fischman D, Baim DS, Leon M, Goldberg S, Hirshfeld JW, Cleman MW, Teirstein PS, Walker C. Restenosis after placement of Palmaz-Schatz stents in native coronary arteries. Initial results of a multicenter experience. *Circulation*. 1992;86:1836–1844.
36. Assali AR, Moustapha A, Sdringola S, Denktas AE, Willerson JT, Holmes DR Jr, Smalling RW. Acute coronary syndrome may occur with in-stent restenosis and is associated with adverse outcomes (the PRESTO trial). *Am J Cardiol*. 2006;98:729–733.